J. Fluid Mech. (1977), *vol.* 82, *part* 4, *pp.* 687–703
Printed in Great Britain

Simple rotational flows

By J. A. SHERCLIFF
Department of Engineering, University of Warwick, Coventry, England

(Received 16 February 1977)

The paper develops and discusses some new additions to the available stock of analytical solutions of the nonlinear equations of fluid motion. The motions are steady, two-dimensional and devoid of viscous or other rotational forces (although such forces must have been significant during any starting process). The fluid density is constant.

The solutions are in two groups, referred respectively to Cartesian and polar co-ordinates. In both the stream function is of *separable* form, i.e. expressible as a product of two functions, each dependent on one co-ordinate. A remarkable variety of motions is revealed. Those that are most significant physically are described as *bends* (rapid transitions from one rectilinear flow to another) or as *loops* (closed, non-circular, vortex-type flows). The effects of boundary layers at walls or instability are not explored.

The paper closes with a mention of some preliminary experiments on loop flows in which all streamlines are ellipses and some discussion of the applicability of bend flows. Generalizations to axisymmetric flows and compressible flows are also mentioned briefly.

1. Introduction

From the early days of analytical fluid mechanics (Lagrange 1781; Stokes 1842) it has been known that the dynamic behaviour of two-dimensional, steady, constant-density, rotational flow can be expressed in terms of the stream function ψ by means of the general condition

$$\nabla^2\psi = f(\psi) \tag{1}$$

in the absence of significant viscous or other rotational forces.

Not many classes of exact general solutions to this equation appear to be known. Attention has been mainly directed to cases where f takes the form $\pm k^2\psi$ (k constant) and (1) becomes a Helmholtz equation. The other main class which has been explored is that where the vorticity and f are constant everywhere and (1) becomes merely a Poisson equation (Batchelor 1967, pp. 537–543). One simple family of such solutions is obtained by taking ψ as any quadratic function of x and y. The streamlines are then similar, concentric conics. These flow patterns are essentially of two kinds: closed *loops* (i.e. ellipses, including circles); or *bends* (i.e. hyperbolas or parabolas) with flow to and from infinity in different directions. The hyperbolic bend flows have common asymptotes, which implies that the velocities tend to infinity at infinity, where the streamlines crowd together. The case of the *rectangular* hyperbola is of course a familiar irrotational flow. Fraenkel (1961) gave a uniformly *rotational* flow lying between perpendicular asymptotes and involving an eddy near the origin.

This paper will be concerned with more general classes of flows, of which the more interesting are again of the two kinds *loops* or *bends*. In one case the streamlines will again be similar conics, but now *confocal* instead of *concentric*. We shall also find that many bend flows asymptote to rectilinear flows at infinity without the velocities increasing without limit.

We shall not discuss the stability of the flows, nor shall we consider whether any boundary layers would separate in the case of small viscosity if the flows were realized in ducts. We shall mainly confine attention to flows where the whole flow field is governed by a single expression (1), as distinct from having different regimes in different places (cf. Hill's spherical vortex).

It is recognized that fluid-mechanical investigations that are based mainly on mathematical forms, as here, are often artificial, because the physical cause–effect process as time passes is usually not adequately represented, but the nonlinear nature of the equations of motion present such difficulties that it would appear to be well worth adding to the stock of known simple solutions, for comparison with observed flows and for contemplation as possible sources of inspiration and understanding.

2. Separable Cartesian solutions

We first look briefly at solutions of (1) which take the form

$$\psi = X(x)\, Y(y), \tag{2}$$

after a suitable choice of axes. It is convenient to replace (1) by

$$\nabla^2\psi = \psi\, g(\psi) \tag{3}$$

so that

$$X''/X + Y''/Y = g, \tag{4}$$

in which a dash denotes appropriate differentiation. Differentiation with respect to x at constant y gives

$$(X''/X)' = g'X'Y$$

and either $X' = 0$ or $(X/X')(X''/X)' = \psi g'$, a function of ψ. Differentiation with respect to y at constant x gives

$$0 = (\psi g')'\, XY'$$

and either $Y' = 0$ or $\psi g' =$ constant $= A$, say. Thus we either have X or Y constant (merely rectilinear shear flows) or

$$g = A\log\psi + B(\text{constant}), \quad f = A\psi\log\psi + B\psi, \tag{5}$$

the general separable solution.

Helmholtz cases ($A = 0$)

Here X and Y take a sinusoidal, exponential, hyperbolic or linear form, e.g.

$$\psi = C\cos kx\cos ly$$

(a regular pattern of rectangular vortex cells), which, by a suitable choice of origin, covers all the doubly sinusoidal cases. The cases where one or both of X and Y is linear, or where X is sinusoidal with Y hyperbolic or exponential (or vice versa) are less interesting. More interest attaches to the cases where X and Y are both exponential

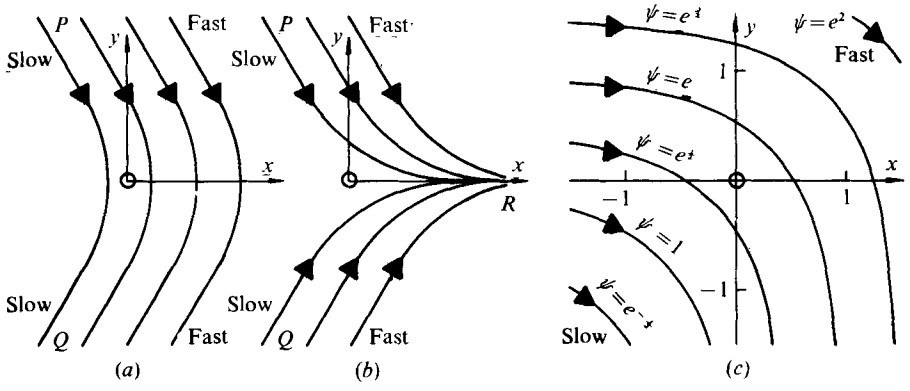

FIGURE 1. Streamlines for the flows (*a*) $\psi = Ce^{kx}\cosh ly$, (*b*) $\psi = Ce^{kx}\sinh ly$ and (*c*) $\psi = C(e^x + e^y)$. (*a*) and (*b*) not to scale.

(or hyperbolic) functions. The doubly exponential form $\psi = C\exp(kx+ly)$ gives a rectilinear flow with an exponential velocity profile, but the cases

$$\psi = C\exp kx \sinh\,(\text{or } \cosh)\, ly$$

have greater novelty, as figure 1 reveals. In each case all streamlines take the same shape; increasing ψ by a factor m shifts a streamline a distance $k^{-1}\log m$ x-wise (in (*a*) or (*b*)). Case (*c*) is a particularly simple case of (*a*), after rotation of the axes.

In regions P and Q the asymptotic flows are rectilinear shear flows (with slow and fast tendencies as indicated) and velocities at infinity are finite. Case (*a*) is a bend flow through an angle $2\tan^{-1}(k/l)$. The bend is quite abrupt because the streamlines approach their asymptotes with exponential vigour. In case (*b*), however, the streamlines have also a common asymptote R where velocities increase without limit. In real fluids compressibility or cavitation would intervene as the pressure dropped there.

The mechanics of case (*a*) or (*c*) make an interesting contrast with irrotational flow round a bend. On the bend there is a centrifugal pressure gradient. In the irrotational flow, Bernoulli's equation therefore requires the fluid to accelerate on the inside of the bend and decelerate on the outside, with corresponding narrowing and widening of the streamtubes. In case (*a*) or (*c*), however, *all* streamtubes widen at the bend as the fluid decelerates, but because Bernoulli's equation contains a quadratic velocity term the faster outer streamlines generate greater pressure rises and the centrifugal gradient can still occur. These ideas also apply to many of the flows which we shall discuss later and which behave very differently from irrotational flow.

Finally we come to the doubly hyperbolic cases:

$$\psi = 4C\cosh\,(\text{or sinh})\, kx \cosh\,(\text{or sinh})\, ly.$$

Where $|kx| \gg 1$ and $|ly| \gg 1$, these become $\psi = C\exp(\pm kx \pm ly)$ with appropriate choices of sign. The flows have diamond-shaped streamlines, with exponential velocity profiles, as indicated in figure 2, except near the axes. At the axes the cases differ: near the x axis (*a*) and (*b*) are like figure 1 (*a*) while (*c*) is like figure 1 (*b*); near the y axis (*a*) is like figure 1 (*a*) while (*b*) and (*c*) are like figure 1 (*b*); near the origin, however, the rectilinear parts of the flows are extinguished, and a stagnation point occurs there in (*c*).

If a portion of case (*a*) well away from the origin is selected, it reveals how bend flows

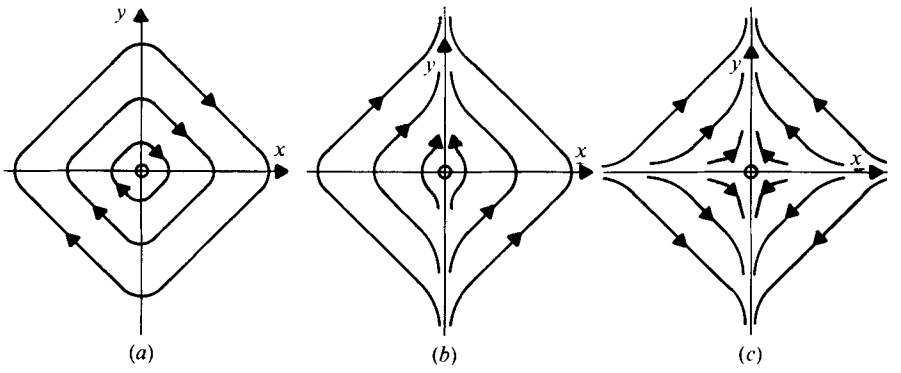

FIGURE 2. Streamlines for the flows (*a*) $\psi = 4C\cosh kx\cosh ly$, (*b*) $\psi = 4C\sinh kx\cosh ly$ and (*c*) $\psi = 4C\sinh kx\sinh ly$ (not to scale).

can follow each other virtually without mutual interference because the exponential settling to rectilinearity is so rapidly completed in each bend. Other convex polygonal flows should be physically possible, with arbitrary bend angles joining rectilinear stretches, each with the same exponential velocity profile. (We are assuming that the part of the flow near to the origin is discarded.) It is the apparent ability of these exponential rectilinear flows to bend swiftly through an arbitrary angle which is their most interesting property. The relevant length scale is the transverse distance over which the velocity rises by $1:e$ in the rectilinear flow. We shall find other flows with similar properties later.

Cases with $A \neq 0$

Equations (4) and (5) imply that

$$X''/X = A\log X + C \quad \text{(constant)},$$

with a similar equation (same A) for Y. This integrates to

$$X'^2 = AX^2\log X + DX^2 + E \quad (D, E \text{ constant}),$$

and

$$x = \pm\frac{1}{2^{\frac{1}{2}}}\int\frac{dz}{((z+Fe^{-z})A)^{\frac{1}{2}}},$$

where $z = 2(\log X + D/A)$ and $F = 2E/A$. $F = 0$ gives $X \propto \exp(\frac{1}{4}Ax^2)$, which combines with the equivalent Y solution to give one of the infinity of flows with concentric circular streamlines. But when $F \neq 0$ for one or both of the X and Y solutions, a great range of cases results. These can be found only by numerical quadrature. Rather than pursue these in detail, we merely state a qualitative classification of the flows in the form of table 1 and figure 3. F_x and F_y are the values of F in the X and Y parts of the solution. The values 0 and $1/e$ prove to be crucial. Figure 3 does not distinguish the x and y axes, either of which may be horizontal, with the other vertical.

Figure 3(*a*) groups the 'U-bends' while figure 3(*b*) groups the closed vortices and figure 3(*c*) groups the right-angle bends. When no straight edge occurs, the flow field is unbounded. Where streamlines share a common asymptote velocities tend to infinity. The $A = 0$ cases (figures 2*a*, *b* and *c*) belong respectively to the groups shown in figures 3(*b*iii), 3(*d*ii) and 3(*c*i).

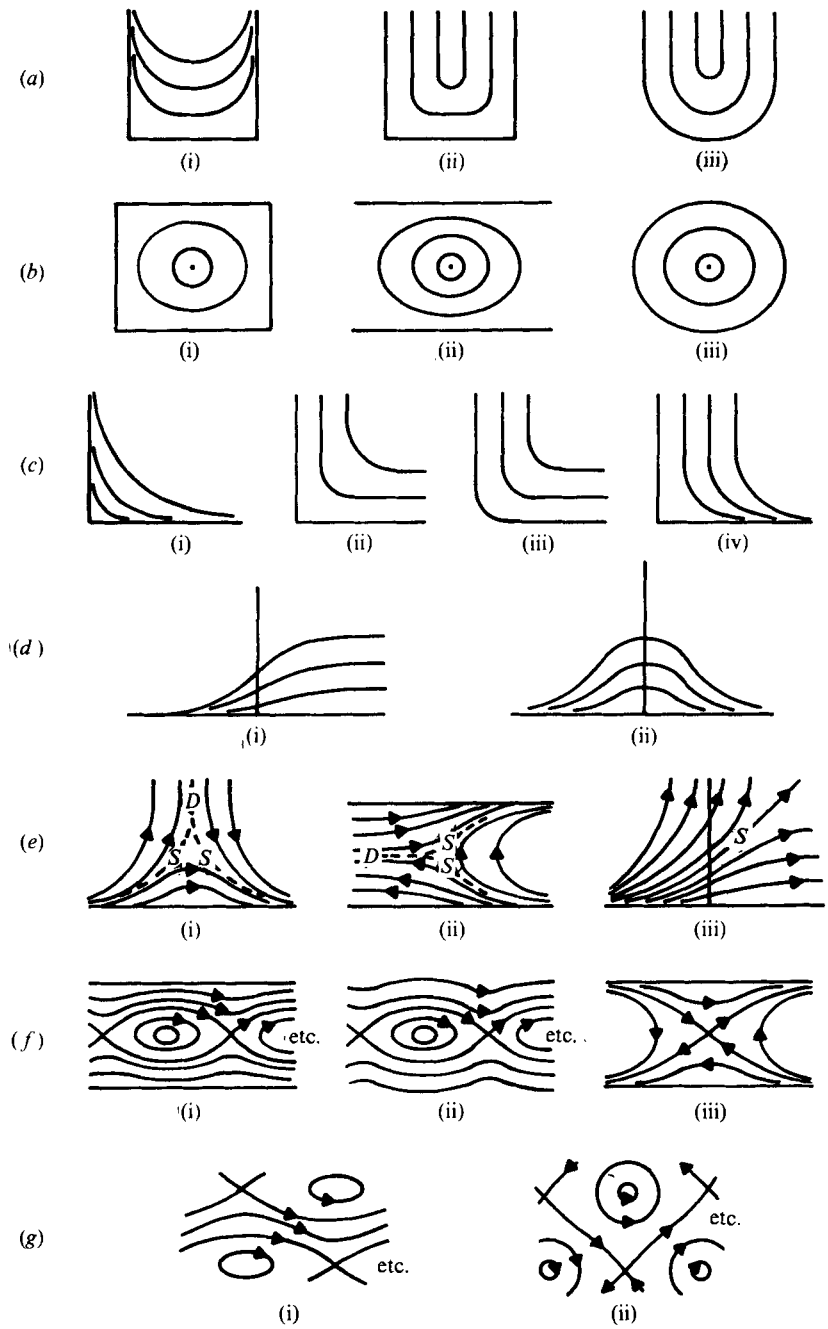

FIGURE 3. Alternative streamline patterns for Cartesian-separable rotational flows ($A \neq 0$) (not to scale). Table 1 lists the conditions for their occurrence.

(*a*) *A positive*

	$F_x \leqslant 0$	$0 < F_x < 1/e$	$F_x = 1/e$	$F_x > 1/e$
$F_y \leqslant 0$	(*b*iii)	(*b*iii), (*f*iii)	(*a*iii), (*e*i)	(*d*ii)
$0 < F_y < 1/e$	(*b*iii), (*f*iii)	(*b*i), (*b*iii), (*f*iii)	(*a*ii), (*a*iii), (*e*i), (*e*ii)	(*a*i), (*d*ii)
$F_y = 1/e$	(*a*iii), (*e*i)	(*a*ii), (*a*iii), (*e*i), (*e*ii)	(*c*ii), (*c*iii), (*e*iii)	(*c*iv), (*d*i)
$F_y > 1/e$	(*d*ii)	(*a*i), (*d*ii)	(*c*iv), (*d*i)	(*c*i)

(*b*) *A negative*

	$F_x < 0$	$F_x = 0$	$0 < F_x < 1/e$
$F_y < 0$	(*b*i)	(*b*ii)	(*f*i)
$F_y = 0$	(*b*ii)	(*b*iii)	(*f*ii)
$0 < F_y < 1/e$	(*f*i)	(*f*ii)	(*g*i), (*g*ii)

TABLE 1. The entries refer to figure 3 numbers.

Figure 3 (*e*) is an unusual group in each member of which a limiting streamline S separates two kinds of flow. In (i) and (ii) the region D locally approaches Couette flow, with the velocity vanishing on the axis of symmetry. A curvilinear *triangle* of streamlines would otherwise be highly suspect! The arrows show a consistent set of flow directions.

Figures 3 (*f*) and (*g*) contain branch points where the velocity is zero. Figures 3 (*f*) repeat indefinitely in one direction while figures 3 (*g*) repeat in both directions. Also figure 3 (*f*i) could be repeated indefinitely in parallel strips and would then contrast with figure 3 (*g*i), with its staggered vortex rows. Figure 3 (*g*ii) is *not* figure 3 (*b*i) rotated through 45°. All the vortices in figures 3 (*b*), (*f*) and (*g*) are not singular at their centres, the vorticity being finite there. Figure 3 (*f*) is very reminiscent of the linearized solutions found by Lautard & Zeytounian (1970).

Enough has now been said to reveal the extraordinary variety of the Cartesian-separable rotational flows.

3. Separable polar solutions

An elegant range of solutions of (1) emerges if we postulate the separable form

$$\psi = R(r)\,H(\theta) \tag{6}$$

in terms of the polar co-ordinates r and θ. Inserted into (3) this gives

$$r^2(R'' + R'/r)/R + H''/H = r^2 g, \tag{7}$$

which differentiated at constant r gives either

$$H' = 0 \quad \text{or} \quad (H/H')(H''/H)' = r^2(g'\psi).$$

Differentiating again at constant θ gives

$$r^2(g'\psi)'\,\psi R'/R + 2rg'\psi = 0$$

and either

$$g' = 0, \quad R' = 0 \quad \text{or} \quad -\frac{(g'\psi)'}{2g'} = \frac{R}{R'r} = \text{constant} = k^{-1}, \quad \text{say,} \tag{8}$$

as can be seen by differentiating again at constant r. From (8) we have

$$R = r^k,$$

if we absorb the constant into H. Equation (8) also yields

$$\tfrac{1}{2}kg'\psi + g = E \quad \text{(constant)}$$

and $$g = E + F\psi^{-2/k} = E + Fr^{-2}H^{-2/k} \quad (F \text{ constant}),$$

which is compatible with (7) if $E = 0$ and if

$$k^2 + H''/H = FH^{-2/k}, \tag{9}$$

the differential equation that determines H. The streamlines are geometrically similar along radial rays from the origin. The solution satisfies (1) in the form

$$\nabla^2\psi = F\psi^n, \quad \text{where} \quad n = 1 - 2/k. \tag{10}$$

These solutions should not be confused with the viscous ones of Moffatt (1964), in which ψ was also of the form $r^kH(\theta)$.

In passing we also noted the alternatives: $H' = 0$, $R' = 0$ or $g' = 0$. The first corresponds to arbitrary concentric circular motions and the second to uniform radial motion. The third case is more significant and corresponds to solutions of the Helmholtz equation

$$\nabla^2\psi = F\psi.$$

Though this corresponds to (10) with $n = 1$, apparently implying that $k \to \infty$, there are now solutions other than the form $R = r^k$. As Lamb (1932, p. 245) points out, R can be a Bessel function, with H sinusoidal. (See also Batchelor 1967, p. 535.) We shall confine attention here to cases where $R = r^k$, which do not appear to have been explored.

If $k \neq 1$, (9) integrates to

$$k^2H^2 + H'^2 - BH^{2(k-1)/k} = C \quad \text{(constant)},$$

where $B = kF/(k-1)$, and so

$$\theta = \pm \int \frac{dH}{(C - k^2H^2 + BH^m)^{\frac{1}{2}}},$$

in which $$m = 2(k-1)/k. \tag{11}$$

If $F \neq 0$, we may simplify by setting $H = h|F/k(k-1)|^{\frac{1}{2}k}$ to get

$$\theta = \pm \frac{1}{k} \int \frac{dh}{(A - h^2 \pm h^m)^{\frac{1}{2}}}, \tag{12}$$

in which $A = (C/k^2)\,|k(k-1)/F|^k$. We discuss the case $k = 1$ later.

In all subsequent work we shall assume that scaling has been done so as to make H and h identical, i.e. $|F/k(k-1)|^{\frac{1}{2}k} = 1$. Then, when streamlines are plotted, we shall plot the line $\psi = 1$.

Classification of the cases

The possible cases cover all combinations of A and k and the sign of the last term under the square root in (12). We shall use the phrases *positive choice* and *negative choice* to distinguish cases under the last item. We shall also consider only situations where h and H are positive. The real, positive value of h^m will always be selected whenever there

are alternatives. If H gets to zero and changes sign, it means that all streamlines have gone to infinity or into the origin and have reappeared in what, from a physical point of view, would be a separate flow which would normally be discarded.

If $F = 0$ the flows are well-known irrotational ones with streamlines of the petal ($k < 0$) or bend ($k > 0$) types, respectively, going into the origin or to infinity (along a common radial asymptote) at distinct values of θ.

When $F \neq 0$, a variety of flows results. For brevity we merely state their classification in table 2. The loop and the bend cases are physically the most significant. Cases for which the two values of k are mutually reciprocal form dual pairs in which the h-integral takes the same form if h is replaced by $|A|^{\frac{1}{2}} h^k$. The extreme value A_0 of $h^2 \mp h^m$ plays a crucial role. In the loop flows the vorticity at the origin is zero if $k > 2$, finite if $k = 2$ and unbounded if $k < 2$.

When $A = 0$, putting $p^2 = h^{m-2} - 1$ leads to $h = |\cos\theta|^k$ (to a suitable θ-origin), i.e. rectilinear flow with velocity $v_y \propto x^{k-1}$. When $A \neq 0$, A becomes negligible as $r \to \infty$ if $k < 1$ (positive choice) and the flow approaches an '$A = 0$' flow. But, if $k > 1$, θ behaves like $h/A^{\frac{1}{2}}$ as $r \to \infty$ and so the streamlines have a common asymptote.

When $k = 1$ we find that

$$\theta = \int \frac{dh}{[A - (h^2 \pm 2\log h)]^{\frac{1}{2}}} \quad \text{if} \quad H = h\,|F|^{\frac{1}{2}}. \tag{13}$$

In table 2 the phrases 'positive choice' and 'negative choice' refer to the signs as written in (13), and $A_0 = 1$ for $k = 1$.

Cases expressible in standard functions

The cases (in addition to $A = 0$) where solutions exist in terms of standard functions are the dual pairs $k = (\frac{1}{2}, 2)$ and $(-\frac{1}{2}, -2)$ and the self-dual case $k = -1$.

The case $k = 2$. These uniform-vorticity solutions have already been mentioned. We find that $\psi/r^2 = h = \pm\frac{1}{2} - (A + \frac{1}{4})^{\frac{1}{2}} \cos 2\theta$, where the plus or minus sign corresponds to a positive or negative choice. The streamlines are *concentric conics*. For

$$0 > A > A_0 = -\tfrac{1}{4}$$

(positive choice), the loop flows are merely ellipses (with two maxima and minima for r per circuit) and *always* close after one circuit, whatever the value of A. For $A > 0$, the bend flows are hyperbolas with common asymptotes $\theta = \pm\frac{1}{2}\tan^{-1}(2A^{\frac{1}{2}})$. They are *concave*, i.e. could lie within an angle less than π between two walls intersecting at the origin. For $A = 0$, the conic becomes two parallel straight lines (Couette flow).

The case $k = \frac{1}{2}$. Here $\frac{1}{2}A - (\frac{1}{4}A^2 \pm 1)^{\frac{1}{2}} \cos\theta = h^2 = \pm\psi^2/r$, and the streamlines are *confocal conics*. The choice of sign under the root corresponds to a positive or negative choice. The bend flows are hyperbolae, each streamline having a different pair of asymptotes. At infinity ψ varies like $x^{\frac{1}{2}}$, if the flow is parallel to the y axis. Either branch of the hyperbola may be chosen and the bend may be *concave* (in the sense just used) or *convex*. The asymptotes are parallel to $\theta = \pm\tan^{-1}(2/A)$. The loop flows all close after one circuit and are ellipses (with a single maximum and minimum for r per circuit) for $A > A_0 = 2$. This case is peculiar in that the velocity is unbounded at the

		$k < 0$	$0 < k \leqslant 1$	$k > 1$
Positive choice	$A > A_0$	0 to ∞*		$A > 0$ bend†
	$A = A_0$	limit circle	bend* († if $k = 1$)	$A = 0$ rectilinear
	$A > A > 0$	petal and bend*	($A = 0$ rectilinear	$0 > A > A_0$ loop
	$A = 0$	rectilinear	unless $k = 1$)	$A \leqslant A_0$ impossible
	$A < 0$	bend*		
Negative choice	$A > 0$	petal	$A > A_0$ loop	$A > 0$ bend†
	$A \leqslant 0$	impossible	$A \leqslant A_0$ impossible	$A \leqslant 0$ impossible

Notes

(i) * indicates finite velocities and distinct streamlines in rectilinear flow at ∞.
(ii) † indicates unbounded velocities and common asymptote at ∞.
(iii) '0 to ∞' indicates that streamlines go from 0 to ∞ over a finite range of θ.
(iv) 'limit circle' indicates that streamlines spiral into a circle from 0 or ∞. (Discarded because streamlines intersect.)
(v) 'petal' indicates that streamlines go to and from 0 over a finite range of θ, with a single maximum for r.
(vi) 'bend' indicates that streamlines go to and from ∞ over a finite range of θ, with a single minimum for r.
(vii) 'rectilinear' indicates shear flow with ψ like x^k, say.
(viii) 'loop' indicates that streamlines oscillate between a maximum and minimum for r, θ increasing monotonically. Of interest only when the loop closes after one circuit (otherwise streamline crossing occurs).

TABLE 2

origin and there is an unbalanced force at this point, i.e. in any physical realization the singularity would have to be replaced by a slender, load-bearing body of confocal-elliptical cross-section. By integrating the pressure round any streamline, with the aid of Bernoulli's equation, this transverse force is found to be

$$\tfrac{1}{2}\pi\rho[C-1)/(C+1)]^{\frac{1}{2}}$$

per unit length, where $C = \frac{1}{2}A$ and ρ is the density.

It is also worth noting that in this case it is possible to surround a finite elliptical region of the rotational flow with an irrotational flow which at infinity is a uniform stream in the y direction. If $\psi = 1$ is the dividing streamline, the velocity at infinity is $\frac{1}{2}[(C-1)/(C+1)]^{\frac{1}{2}}$. The transverse force can of course be calculated alternatively from the Zhukhovskii circulation/lift theorem. There is a detached stagnation point at $\theta = 0$, $r = 2C^2/(C^2-1)^{\frac{1}{2}}$. The complex potential for the irrotational flow is given parametrically by

$$\phi + i\psi = i + \tfrac{1}{2}C\{e\sin 2\zeta - 2\zeta\},$$

where $z = x+iy = (\cos\zeta + iD\sin\zeta)^2/C(1-e)$, $e = (1-C^{-2})^{\frac{1}{2}}$ (the eccentricity of the ellipse) and $D = [(1-e)/(1+e)]^{\frac{1}{2}}$. ($\zeta$ real corresponds to $\psi = 1$.)

The cases $k = -1, -2, -\frac{1}{2}$. These cases can be expressed in terms of elliptic integrals of the first kind. Some details are given in the appendix. However, as extensive computing has to be done to explore the other cases, it is simpler to treat these cases in the same way. (The cases $k = \frac{1}{4}, \frac{1}{3}, \frac{2}{3}, \frac{3}{4}, \frac{3}{2}, \frac{4}{3}$, 3, 4 can be expressed in terms of elliptic integrals of the *third* kind, but the value of this procedure is even more dubious.) If $F = 0$, irrotational petal flows result, and $k = -1$, -2 and $-\frac{1}{2}$ give respectively

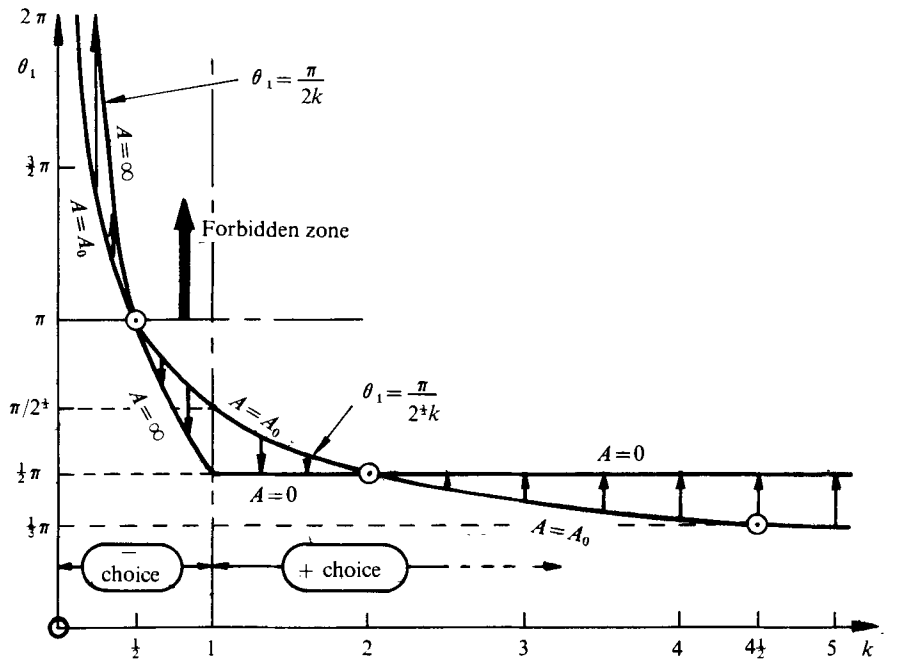

FIGURE 4. Loop flows: the variation of θ_1 with k and A. The arrows indicate the trend as A increases over the permissible range.

streamlines which are paired circles (through the origin: a dipole flow), Bernoulli's lemniscate and the cardioid. The limit-circle cases can also be simply solved:

$$h = \begin{cases} 2^{-\frac{1}{2}} \tanh(\theta/2^{\frac{1}{2}}) & \text{for } k = 1 \quad (A = A_0 = \frac{1}{4}), \\ \tanh^2\theta - \frac{1}{3} & \text{for } k = -2 \quad (A = A_0 = \frac{4}{27}), \\ [\frac{1}{2}(3\tanh^2\frac{1}{2}\theta - 1)\,3^{\frac{1}{2}}]^{\frac{1}{2}} & \text{for } k = -\frac{1}{2} \quad (A = A_0 = -2/3^{\frac{3}{2}}). \end{cases}$$

In each case tanh can be replaced by coth, to yield the other branch.

Loop flows

Here the important quantity is θ_1, the difference between the values of θ at which the denominator in (12) vanishes. For a closed loop we require $\theta_1 = \pi \div (\text{integer})$. In fact $\theta_1 \to \pi/(2k)^{\frac{1}{2}}$ as $A \to A_0$, $\theta_1 \to \frac{1}{2}\pi$ as $A \to 0$ $(k > 1)$ and $\theta_1 \to \pi/2k$ as $A \to \infty$ $(0 < k < 1)$. Figure 4 reveals what closed loops are possible. $k = 2$ or $\frac{1}{2}$ each gives only one value of θ_1 and these values are not available for other values of k. k large implies velocity variation so extreme as to be rather unlikely.

Figure 5 gives the results of computations to find the pairs of values of A and k which yield closed loops. As $-A$ decreases, the streamline shape changes from a circle towards a polygon, with very abrupt bends joining rectilinear stretches, behaviour reminiscent of that discussed in § 2. Figure 6 shows a portion of such cases for $\theta_1 = \frac{1}{3}\pi$ and $\frac{1}{4}\pi$.

Bend flows

Here the important quantity is θ_0, the bend semi-angle, i.e. the difference between those values of θ at which $r \to \infty$ and reaches its minimum. Figure 7 summarizes the

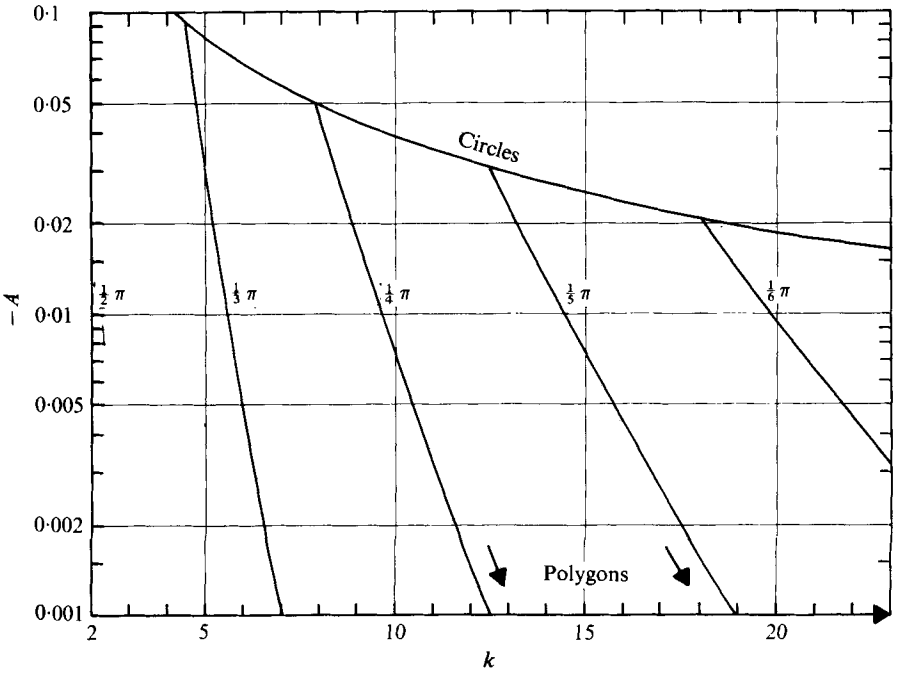

FIGURE 5. Loop flows: the values of A and k for which the streamlines form closed loops after one circuit of the origin.

results of extensive computations to find θ_0 as a function of A and k. Values of θ_0 greater than π are of no interest because of streamline crossing. As $A \to \infty$, if $k > 0$, $\theta_0 \to \pi/2k$. The figure includes the case $k = 1$, even though this is singular and does not fit into the smooth sequence of the other cases.

The singular case $k = 0$ does however fit into the smooth sequence, as the figure reveals, even though it is not physically realizable. When $|k|$ is very small and $|m|$ very large, in the quantity

$$Q = A - h^2 + h^m$$

the term h^2 is significant only when h is near 1, and so we may replace it by 1. Then $Q = A - 1 + h^m = p^2$, say, and

$$\theta = \frac{2}{mk} \int \frac{dp}{[p^2 + (1-A)]^{(m-1)/m}} \approx \int \frac{dp}{p^2 + 1 - A}.$$

Hence
$$p \approx (1-A)^{\frac{1}{2}} \cot[(1-A)^{\frac{1}{2}}\theta]$$

and on the streamline $\psi = 1$

$$r \approx (1-A)^{\frac{1}{2}} \operatorname{cosec}[(1-A)^{\frac{1}{2}}\theta].$$

The bend semi-angle $\theta_0 = \pi/2(1-A)^{\frac{1}{2}}$. Cases where this approach fails because A is near 1 are of no interest because θ_0 is too large.

The insensitivity of θ_0 to the value of k in the range $0 > A > -1$ is quite remarkable.

Figure 8 shows specimen streamlines for various cases where $\theta_0 = \frac{1}{4}\pi$ or $\frac{3}{4}\pi$, i.e. concave and convex right-angle bends. The convex bends occur only for $k < \frac{2}{3}$. As $k \to -\infty$, each convex bend streamline becomes a quarter-circle (centred at 0) joining two rectilinear stretches, and each concave bend streamline becomes an instant bend

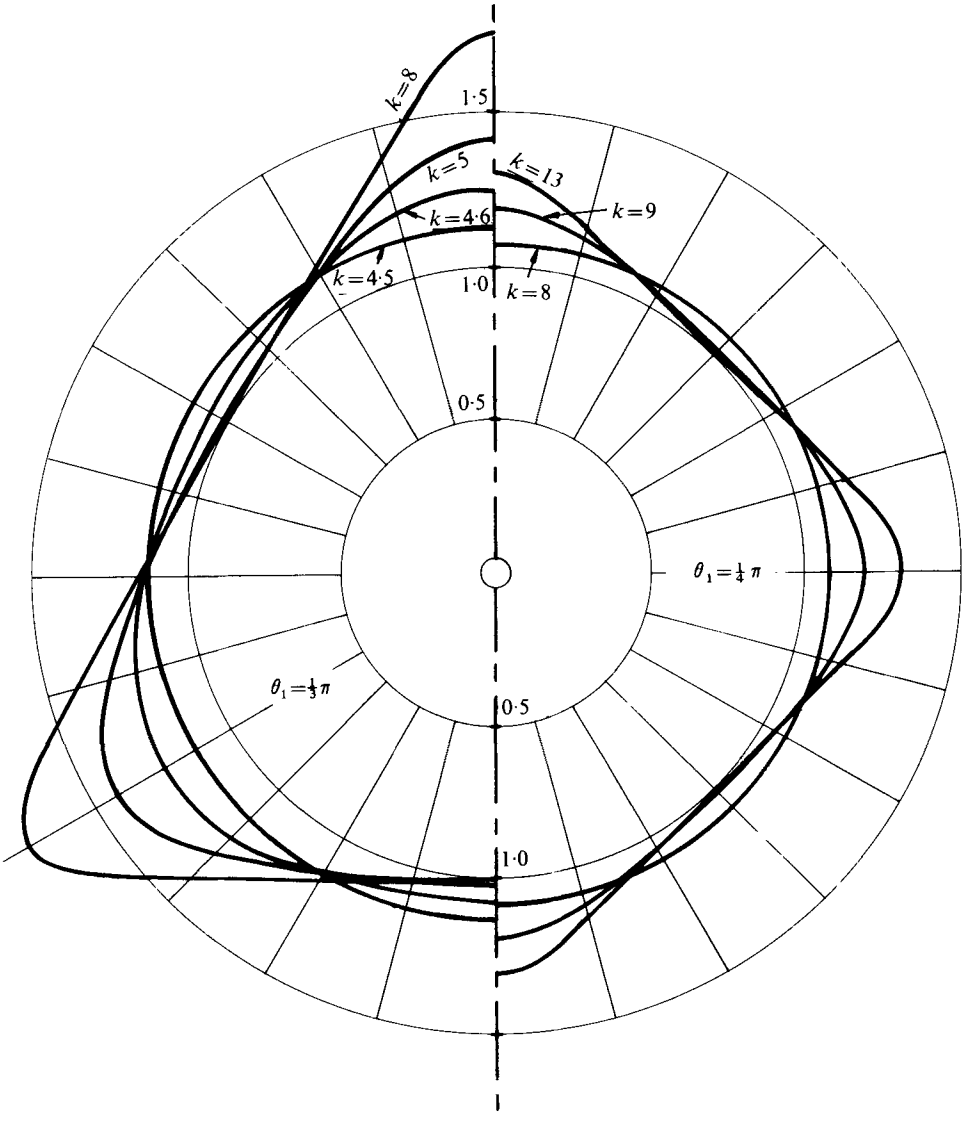

FIGURE 6. Loop flows: portions of streamlines for $\theta_1 = \frac{1}{3}\pi$ and $\frac{1}{4}\pi$, showing the trend from circular to triangular or square form. (These curves are the lines $\psi = 1$ in the case where $|F/k(k-1)|^{\frac{1}{2}k} = 1$.)

joining two rectilinear stretches. This behaviour can be confirmed analytically. Figure 8 includes only those bends that have distinct streamlines (and so finite velocities) at infinity. Note that the concave bends are ones where the fluid slows down in the bend, as in the bend flows in figure 1. A difference from figure 1 is that a rectilinear flow in which $\psi \propto x^k$, say, can bend either way (i.e. towards or away from its high velocity side), following the solutions presented here, but the rectilinear flow in figure 1, where $\psi \propto e^{kx}$, say, can bend only towards its low velocity side, following the solutions presented in § 2. It perhaps needs emphasizing that this is a mathematical result; fluid forced along a bent duct will go round a bend either way, but not following the solutions presented here.

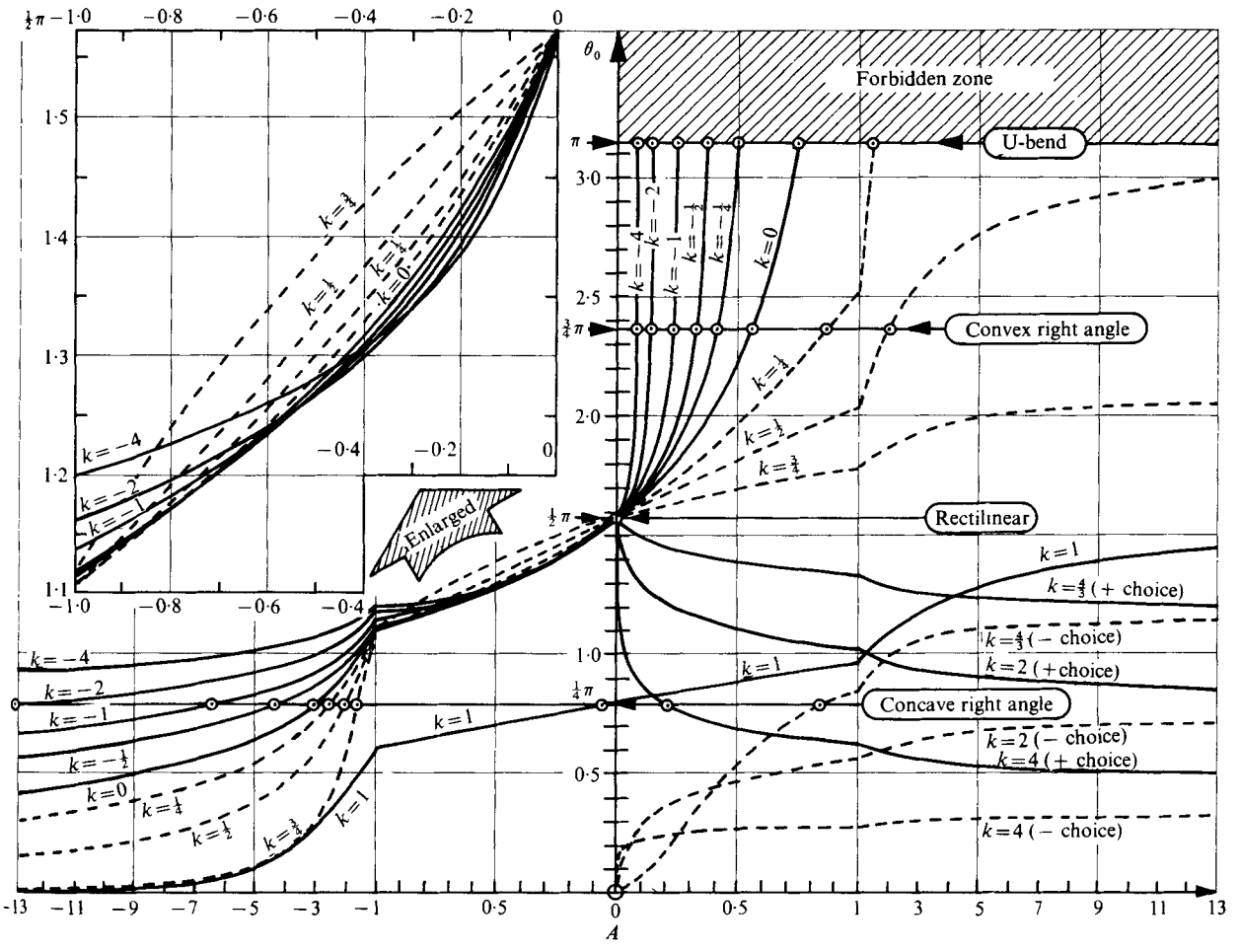

FIGURE 7. Bend flows: the variation of θ_0 with k and A. Note the changes of scale at $A = \pm 1$ and the enlarged version of the curves for $-1 \leqslant A \leqslant 0$ in the top left-hand corner, necessary to distinguish them.

In figure 8, in the rectilinear flow on either side of each bend $\psi \propto x^k$, if x is the distance from the parallel axis, and $v_y \propto x^{k-1}$, where $k-1$ is negative in all cases. Thus the velocities are highest on those streamlines nearest to the origin.

Another point to note is that the rapidity with which the rectilinear flow is approached on either side of the bend begins to fall off greatly once k rises past zero (e.g. see $k = 0{\cdot}65$ curve), while for k negative the adjustment is swift, as for the exponential bend flows in § 2.

Realization and application of bend flows

The bend flows discussed here could in principle be produced experimentally, provided that instabilities, boundary-layer separation or secondary flows did not set in so rapidly downstream as to preclude all observation of the desired flow. The flows could emerge from an upstream system for generating the appropriate vorticity distribution, before being deflected by correctly shaped walls.

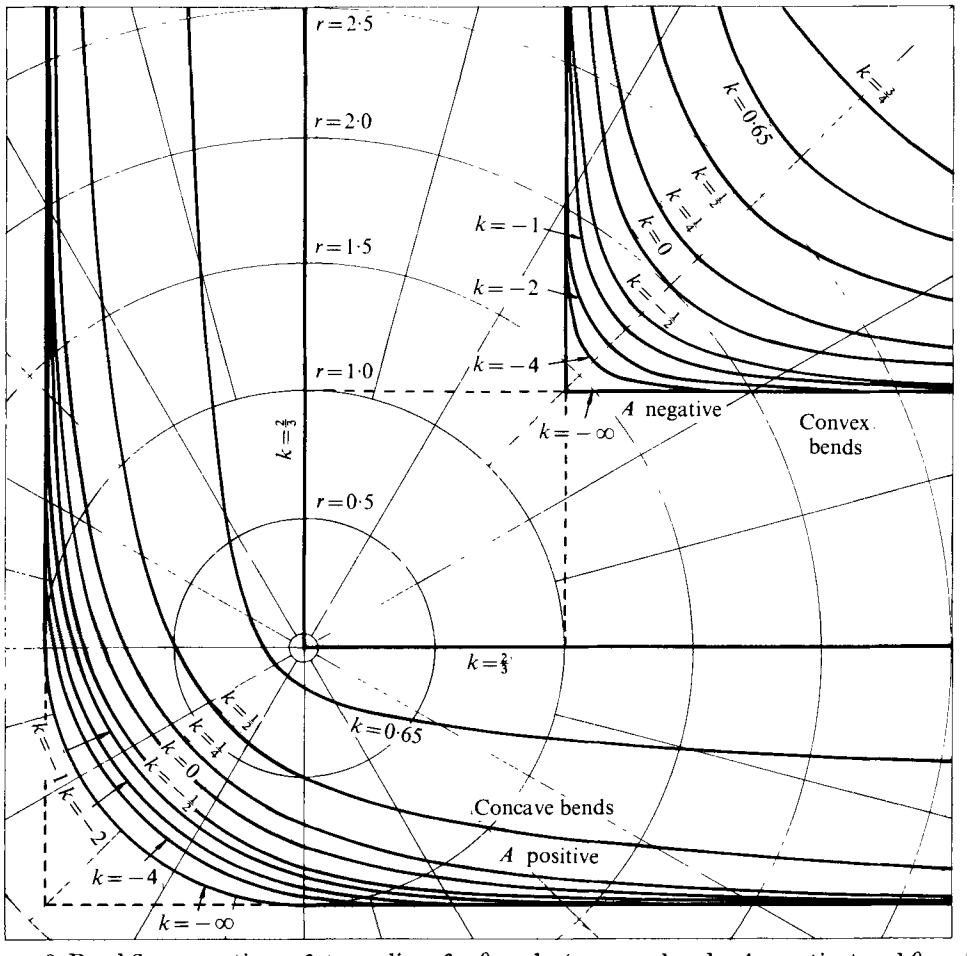

FIGURE 8. Bend flows: portions of streamlines for $\theta_0 = \frac{1}{4}\pi$ (concave bends, A negative) and $\theta_0 = \frac{3}{4}\pi$ (convex bends, A positive). These curves are the lines $\psi = 1$ in the case where $|F/k(k-1)|^{\frac{1}{2}k} = 1$.

It would be interesting, for instance, to experiment with ducted bend flows for which $k = -1$, where a portion ($x > 0$) of rectilinear flow in which the velocity varies like x^{-2}, x being transverse to the stream, could be bent through 90°, say, towards either higher or lower x. One imagines that separation would be most delayed in the latter case, a 'convex' bend in which the pressure falls as the bend is entered. It remains to be seen whether such flows are well enough behaved to be of practical engineering interest, and whether the presence of vorticity makes the stream more easily deflected, as the mathematics might suggest. It is conceivable that the flows might find application in situations such as VTOL aviation where swift deflexion of a jet by the introduction of curved walls into the stream is required, particularly if the need for turning vanes internal to the stream could be eliminated. The penalty would be the need for vorticity to be introduced into the stream, although this might readily be made to result from the upstream devices producing the flow. A non-uniform jet has less thrust per energy content, however, and vorticity generation by *dissipative* processes is undesirable in a power application. Non-uniform heat release might be a more attractive proposition.

The theoretical work presented here can readily be extended. For instance, there are axisymmetric analogues in cylindrical or spherical polar co-ordinates with azimuthal vorticity rings. Physically the axisymmetric flows are rather more interesting than the two-dimensional ones because the vorticity-stretching mechanism is active and (vorticity) ÷ (distance from axis) is now $f(\psi)$, ψ being Stokes's stream function. They might also be easier to produce experimentally than two-dimensional flows, which involve side walls. Their scope is somewhat more limited however because intersections of streamlines with the axis are excluded as distributed sources are physically unacceptable. It does not appear to be possible analytically to integrate the second-order differential equation that is analogous to (9) in general, however, although the case where $\psi = rh(\theta)$ is tractable. Some axisymmetric rotational flows are of course well known. Hill's spherical vortex is a compound flow, made up from two flow regimes.

A further extension of the two-dimensional polar solutions is possible: to rotational compressible perfect gas flow, where in compliance with Crocco's theorem there are variations in stagnation enthalpy or entropy or both. The stream function ψ now refers to mass flow, not volume flow, and each of the quantities (vorticity/density), stagnation enthalpy and entropy is proportional to an appropriate power of ψ. The physical interest here arises because thermodynamic processes (combustion, shocks, etc.) offer the possibility of producing controlled distributions of vorticity of the kind discussed in this paper.

Experiments on loop flows

Some preliminary experiments have been conducted on the two kinds of elliptical loop flows with $k = \frac{1}{2}$ or 2. The concentric-elliptical flows ($k = 2$) can easily be produced for limited periods by steadily rotating a cylindrical tank of elliptical cross-section full of water about an axis through its centre parallel to its generators, until the water is rotating like a solid body, and then rapidly stopping the tank. A Perspex tank with major and minor axes of 420 and 280 mm and a distance of 150 mm between its plane ends has been employed, rotating at speeds of up to a quarter of a revolution per second. It has been found that the elliptical motion when the tank is stopped is very stable and persists for a few revolutions before it is progressively disrupted by a combination of secondary flow (due to the boundary layers on the plane walls) and weak turbulence originating in the boundary layers. (The same agencies also establish the initial steady motion in the rotating tank.) The readiness of the fluid to move with uniform vorticity is of course to be expected in view of Batchelor's (1956) results. Figure 9 (plate 1) shows some of the results, achieved by the hydrogen-bubble technique. It is easily shown that the flows with $k = 2$ have particularly simple kinematic properties, whereby uniform rotation is combined with a deformation rate whose principal axes are always at 45° to the axis of the ellipse. A key feature is that the rotation time of a fluid element is also its orbit time, just as in the original solid-body rotation, and so radial lines stay radial, while they shorten and extend periodically. This particular experiment and its variants obviously have considerable potential for educational purposes.

First attempts to produce confocal ($k = \frac{1}{2}$) elliptical flows in the same tank by generating swirling flows with a tangential inlet at the periphery and a perforated, tubular sink at the focus, capable of carrying the side force, have revealed that realizing such motions will be a very difficult assignment. The turbulence tends to make the flows cling to what can only be called Batchelor (1956) behaviour, i.e. they tend to

maintain uniform mean vorticity and therefore approximate more closely to the concentric ($k = 2$) elliptical flows.

Appendix. Bend cases expressible in terms of elliptic integrals of the first kind, $F(\phi, K)$

Here K is used instead of k, which in this paper has a different significance.

(*a*) *The case* $k = -1$. Here

$$\theta = \int_h^\infty \frac{dh}{(h^4 - h^2 + A)^{\frac{1}{2}}}.$$

Along the streamline $\psi = 1$, $r = h$.

(i) If A is positive ($< \frac{1}{4}$), $\theta = (1+K^2)^{\frac{1}{2}} F(\phi, K)$, where

$$h^2(1+K)^2 = \operatorname{cosec}^2\phi, \quad A^{\frac{1}{2}} = K/(1+K^2).$$

(ii) If A is negative, $\theta = (1-2K^2)^{\frac{1}{2}} F(\phi, K)$, where

$$h^2(1-2K^2) = \operatorname{cosec}^2\phi - K^2, \quad (-A)^{\frac{1}{2}} = K(1-K^2)^{\frac{1}{2}}/(1-2K^2).$$

The right-angle bends occur with $A = 0{\cdot}228$ and $-6{\cdot}40$. θ_0 is given by $\phi = \frac{1}{2}\pi$.

(*b*) *The case* $k = -2$. Here

$$\theta = \frac{1}{2}\int_h^\infty \frac{dh}{(h^3 - h^2 + A)^{\frac{1}{2}}}.$$

Along the streamline $\psi = 1, r = h^{\frac{1}{2}}$. Let a be the largest (or only) root of $Z^3 - Z^2 + A = 0$.

(i) If A is positive ($< \frac{4}{27}$), $\theta = p^{-\frac{1}{2}} F(\phi, K)$, where $\phi = \frac{1}{2}\pi$ gives θ_0 and

$$p = \tfrac{1}{2}\{3a - 1 + [(1-a)(1+3a)]^{\frac{1}{2}}\} = (h-a)\tan^2\phi, \quad K^2 = 2 - (3a-1)/p.$$

(ii) If A is negative, $\theta = \frac{1}{2}p^{-\frac{1}{2}} F(\phi, K)$, where ϕ ranges from 0 to π, $\phi = \pi$ gives θ_0 and

$$p = [a/(3a-2)]^{\frac{1}{2}} = (h-a)\tan^2\tfrac{1}{2}\phi, \quad K^2 = \tfrac{1}{2} - (3a-1)/4p.$$

The right-angle bends occur with $A = 0{\cdot}142$ and $-13{\cdot}2$.

(*c*) *The case* $k = -\frac{1}{2}$. Here

$$\theta = 2\int_h^\infty \frac{dh}{(h^6 - h^2 + A)^{\frac{1}{2}}}.$$

Along the streamline $\psi = 1$, $r = h^2$.

(i) If A is positive ($< 2/3^{\frac{3}{2}}$), let a be the middle root of $Z^3 - Z^2 + A^2 = 0$. Then $\theta = 2p^{-\frac{1}{2}}(F(\phi, K) - F(\phi_0, K))$, where ϕ ranges from ϕ_0 to $\frac{1}{2}\pi$, $\phi = \frac{1}{2}\pi$ gives θ_0, $p = [(1+3a)(1-a)]^{\frac{1}{2}}$, $\tan\phi_0 = [(a+p-1)/2a]^{\frac{1}{2}}$ and

$$K^2 = \tfrac{1}{2} + (3a-1)/2p, \quad A/h^2 = a - \tfrac{1}{2}(3a+p-1)\cos^2\phi.$$

(ii) If A is negative and $> -2/3^{\frac{3}{2}}$, let a be the largest root of $Z^3 + Z^2 - A^2 = 0$. Then $\theta = 2p^{-\frac{1}{2}} F(\phi, K) - F(\phi_0, K))$, where ϕ ranges from ϕ_0 to 0, $\phi = 0$ gives θ_0,

$$p = \tfrac{1}{2}\{3a + 1 + [(a+1)(1-3a)]^{\frac{1}{2}}\}, \quad \tan\phi_0 = [a/(2a+1-p)]^{\frac{1}{2}}$$

and

$$K^2 = (3a+1)/p - 1, \quad -A/h^2 = a - (3a+1-p)\sin^2\phi.$$

(iii) If A is negative and $< -2/3^{\frac{3}{2}}$, let a be the only root of $Z^3+Z^2-A^2=0$. Then $\theta = p^{-\frac{1}{2}}F(\phi_0, K)-F(\phi, K))$, where ϕ ranges from ϕ_0 to 0, $\phi = 0$ gives θ_0,

$$p = [a(3a+2)]^{\frac{1}{2}}, \quad \tan\tfrac{1}{2}\phi_0 = (a/p)^{\frac{1}{2}}$$

and

$$K^2 = \tfrac{1}{2}+(1+3a)/4p, \quad -A/h^2 = a-p\tan^2\tfrac{1}{2}\phi.$$

The right-angle bends occur at $A = 0{\cdot}324$ and $-4{\cdot}36$.

REFERENCES

Batchelor, G. K. 1956 *J. Fluid Mech.* **1**, 177.

Batchelor, G. K. 1967 *An Introduction to Fluid Dynamics*. Cambridge University Press.

Fraenkel, L. E. 1961 *J. Fluid Mech.* **11**, 400.

Lagrange, J.-L. 1781 *Nouv. Mém. Acad. Berlin.* (See also *Oeuvres*, vol. 4, p. 720.)

Lamb, H. 1932 *Hydrodynamics*, 6th edn. Cambridge University Press.

Lautard, J.-J. & Zeytounian, R. 1970 *C. R. Acad. Sci. Paris* A **271**, 469.

Moffatt, H. K. 1964 *J. Fluid Mech.* **18**, 1.

Stokes, G. G. 1842 *Trans. Camb. Phil. Soc.* **7**. (See also *Papers*, vol. 1, p. 15.)